

Molecular Physics

An International Journal at the Interface Between Chemistry and Physics

ISSN: (Print) (Online) Journal homepage: https://www.tandfonline.com/loi/tmph20

Incorporating reduced axis system embedding into ab initio tunnelling-rotation Hamiltonians with curvilinear vibrational Møller-Plesset perturbation theory

P. Bryan Changala

To cite this article: P. Bryan Changala (17 Jan 2024): Incorporating reduced axis system embedding into *ab initio* tunnelling-rotation Hamiltonians with curvilinear vibrational Møller–Plesset perturbation theory, Molecular Physics, DOI: 10.1080/00268976.2024.2304098

To link to this article: https://doi.org/10.1080/00268976.2024.2304098





FESTSCHRIFT IN HONOUR OF PROF. ATTILA G. CSÁSZÁR



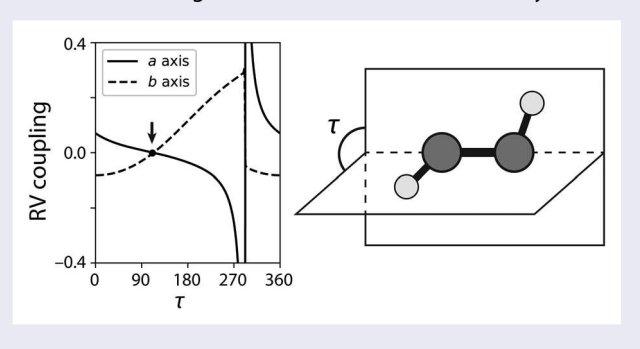
Incorporating reduced axis system embedding into ab initio tunnelling-rotation Hamiltonians with curvilinear vibrational Møller-Plesset perturbation theory

P. Bryan Changala 📵

Center for Astrophysics | Harvard & Smithsonian, Cambridge, MA, USA

ABSTRACT

Large-amplitude vibrational motion influences the rovibrational structure of molecules that tunnel between multiple wells. Reaction path (RP) Hamiltonians, and curvilinear coordinates more generally, are useful for modelling pure vibrational motion in these systems and provide a practical framework for calculating accurate ab initio anharmonic vibrational energies and tunnelling splittings with perturbation theory. These computational tools also offer the means to address rotationvibration coupling associated with large-amplitude motion in rotating molecules. In this paper, we incorporate the reduced axis system (RAS) frame embedding with RP Hamiltonians and second-order vibrational Møller-Plesset perturbation theory (VMP2). Because the RP-RAS Hamiltonian eliminates rotation-vibration momentum coupling everywhere along a one-dimensional reaction path, it is well suited for rovibrational VMP2 methods, the convergence of which relies critically on approximate vibration-vibration and vibration-rotation separability. The accuracy of this combined RP-RAS-VMP2 scheme is demonstrated by comparisons with numerically exact variational calculations and VMP2 parameters based on traditional Eckart embeddings for reduced-dimension models of torsional tunnelling in hydrogen peroxide and inversion tunnelling in cyclopropyl radical. The favourable computational scaling of VMP2 makes it a promising strategy for calculating accurate tunnelling-rotation parameters for medium-sized and larger molecules in full dimensionality.



ARTICLE HISTORY

Received 1 December 2023 Accepted 5 January 2024

KEYWORDS

Tunnelling; perturbation theory; rovibrational structure; spectroscopy

1. Introduction

Molecules that tunnel between local energy minima pose a unique challenge for theoretical calculations of rovibrational spectroscopic parameters. Because the timescale of large-amplitude vibrational motion can be comparable to rotational motion, successful models of tunnelling systems must simultaneously address both highly anharmonic vibrations and strong rotation-vibration coupling, while also balancing computational accuracy and cost for high-dimensional problems.

Curvilinear second-order vibrational Møller-Plesset perturbation theory (VMP2) is an efficient and general method for calculating anharmonic vibrational frequencies and energy splittings of tunnelling molecules [1]. Building on applications of isomerisation reaction path (RP) Hamiltonians [2] in other closely related vibrational mean-field-based studies [3–5], curvilinear VMP2 models have more recently been used with several prototypical examples of large-amplitude vibrational motion including H₂O₂ [6], CH₃NO₂ [1], and gauche-1,3-butadiene [7]. Although the VMP2 rovibrational parameters (i.e. rotational constants, tunnelling splittings, and tunnelling-rotation Coriolis constants) calculated in these studies were found to be of sufficient



accuracy for spectroscopic and structure-determination applications, the factors influencing the performance of rovibrational VMP2 for large-amplitude motion, particularly the choice of molecule-fixed frame, remain incompletely understood.

This paper investigates the combination of the reduced axis system (RAS) [8] with RP VMP2 calculations to generate rovibrational spectroscopic parameters for tunnelling molecules. The primary benefit of the RAS frame is that it eliminates vibration-rotation momentum coupling exactly along a one-dimensional contour, taken here to be the intrinsic isomerisation reaction path. In Section 2, we review briefly the general rovibrational VMP2 framework and how it is combined with a RP-RAS Hamiltonian. The success of this scheme is then demonstrated with reduced-dimension models of two important tunnelling molecules, hydrogen peroxide (H_2O_2) and cyclopropyl radical (c-C₃H₅). We show that the RAS embedding provides a systematic improvement of the accuracy of rovibrational parameters compared to various single-reference Eckart-frame embeddings. Owing to the modest computational scaling of VMP2 methods [9–11], the RP-RAS framework is a promising general approach for quantitative ab initio tunnellingrotation predictions for large molecules.

2. Methods

2.1. Rovibrational VMP2 Hamiltonians

We construct tunnelling-rotation effective Hamiltonians using a rovibrational extension of curvilinear VMP2 described in Ref. [1]. Briefly, a zeroth-order vibrational wavefunction is formed by a simple Hartree product,

$$\Psi(\mathbf{q}) = \phi_1(q_1)\phi_2(q_2)\phi_3(q_3)\dots,$$

where $\mathbf{q} = (q_1, q_2, \ldots)$ are arbitrary, curvilinear internal coordinates. This product wavefunction is variationally optimised, leading to the well known vibrational self-consistent field (VSCF) equations [12, 13]. The one-dimensional VSCF 'modals', $\phi_i(q_i)$, and their corresponding virtual wavefunctions form a complete, orthonormal, anharmonic vibrational basis set. In our implementation, we expand the $\phi_i(q_i)$ modals with an underlying discrete variable representation (DVR) basis set and evaluate all vibrational integrals using the usual DVR quadrature approximation [14]. The potential energy surface (PES) and rovibrational kinetic energy operator (KEO) therefore only need to be evaluated numerically over a discrete grid in **q** space.

The VSCF zeroth-order solution is exact in the limit of completely uncorrelated vibrations. The effects of weak vibrational correlation can be efficiently recovered by

VMP2, i.e. second-order Rayleigh-Schrödinger perturbation theory within the configuration space of virtual VSCF modals [9-11, 15]. By folding in the rovibrational and rotational KEO terms into the perturbation procedure, effective rotational Hamiltonians (or multi-state rovibrational Hamiltonians) are constructed [1], in much the same way as in standard second-order vibrational perturbation theory (VPT2) [16, 17] based on a harmonic oscillator-rigid rotor zeroth-order model of the Watson Hamiltonian [18].

The accuracy of the rovibrational VMP2 predictions relies on the separability of the vibrational degrees of freedom from each other and rotations. Fortunately, the VSCF-VMP2 scheme does not require any particular choice of vibrational coordinate system or frame embedding, which are together defined by the functions $\vec{x}_a(\mathbf{q})$ that specify the Cartesian positions of each atom a in the molecule-fixed frame. (It is assumed that $\vec{x}_a(\mathbf{q})$ are always in a centre-of-mass frame.) The internal coordinate system and frame embedding can thus be chosen to minimise vibration-vibration coupling and vibrationrotation coupling, respectively. For semi-rigid molecules, which undergo small-amplitude displacements from a single equilibrium geometry, normal mode coordinates calculated by the traditional GF method [19] (be they defined with respect to either rectilinear or curvilinear displacements) are a good internal coordinate system because the harmonic normal mode Hamiltonian is vibrationally separable, while the Eckart axis system [20] is a good choice of frame because it approximately decouples vibrations and rotations near the equilibrium geom-

More sophisticated coordinate systems and frame embeddings are required to achieve approximately separable vibrations and rotations for large-amplitude tunnelling molecules, which are of interest in this paper. We turn to a RP coordinate system to minimise pure vibrational coupling and a RAS frame embedding to minimise vibration-rotation coupling. These two pieces of the RP-RAS Hamiltonian are discussed in the following sections.

2.2. RP coordinate system

The RP coordinates (s, \mathbf{d}) are defined with respect to an arbitrary set of n 'primitive' internal coordinates, $\mathbf{q} =$ $(q_1, q_2, \dots, q_n)^T$ (e.g. valence bond or Z-matrix coordinates), via the non-linear transformation

$$\mathbf{q}(s,\mathbf{d}) = \mathbf{r}(s) + \mathbf{T}(s)\mathbf{d},$$

where s is the reaction path arc-length, and $\mathbf{d} =$ $(d_1, \ldots, d_{n-1})^T$ are the n-1 orthogonal normal modes whose displacement vectors are defined by the $n \times (n -$

1) matrix T(s) at each point along the path. The reaction path contour $\mathbf{q}(s, \mathbf{d} = 0) = \mathbf{r}(s)$ satisfies the usual steepest descent (or ascent) equation [2],

$$\frac{d\mathbf{r}(s)}{ds} = \pm \frac{\mathbf{Gf}}{\sqrt{\mathbf{f}^T \mathbf{Gf}}},\tag{1}$$

where \mathbf{f} is the potential energy gradient with respect to **q**, and **G** is the vibrational block of the inverse curvilinear metric tensor [19, 21]. It is convenient to find path solutions to Equation (1) by first reparameterising $\mathbf{r}(s)$ as a function of one the primitive internal coordinates themselves. This proxy coordinate, q^* , is chosen to be that which most closely resembles the path, e.g. the dihedral angle associated with large-amplitude torsional motion. The derivatives $d\mathbf{r}(q^*)/dq^*$ are derived from Equation (1) and the chain rule applied to the identity $r^*(s(q^*)) = q^*$. For the applications below, a numerical solution for $\mathbf{r}(q^*)$ is approximated by a cubic spline function. A fixed number of spline nodes are placed equidistantly in q^* between two fixed boundary points (usually stationary points of the PES). The initial guess value for $\mathbf{r}(q^*)$ at the interior nodes is a simple linear interpolation between the boundary points. The node values are then iteratively refined using a local quadratic approximation of Equation (1) about each node point, updating it via a Newton-like method [22]. We find that this iterative spline solution rapidly converges in as few as one or two iterations (depending on the choice of primitive coordinates).

Once the reaction path curve $\mathbf{r}(q^*)$ is calculated, the orthogonal normal mode displacement vectors $\mathbf{T}(q^*)$ are derived using the orthogonally projected Hessian along the path [2, 21, 23]. In practice, we calculate $T(q^*)$ at, say, 10 to 20 equally spaced positions, and then fit these with a power or Fourier series with respect to q^* . The orthogonal normal mode coordinates d_i are scaled as dimensionless normal coordinates, i.e. those in which the harmonic potential energy curve is $\frac{1}{2}\omega_i d_i^2$, where ω_i is the projected harmonic frequency of the mode. This definition ensures that the VSCF product wavefunction, $\Psi = \phi_0(q^*)\phi_1(d_1)\phi_2(d_2)\dots$, implicitly accounts for the adiabatic change of the orthogonal normal mode frequencies along the reaction path even though the orthogonal wavefunctions $\phi_i(d_i)$ have no explicit dependence on q^* .

The RP coordinate system smoothly interpolates between the conventional normal modes of each stationary point along the path. For periodic paths (e.g. an internal rotation), each segment of the reaction path is bounded by two stationary points (one saddle point and one local minimum), and these two points are used as the fixed boundary condition of the cubic spline solution for each segment. For aperiodic coordinates (e.g. a double-well inversion motion), the segments of the path

between stationary points are uniquely defined, but the terminal segments do not have a unique choice of boundary point. In this case, we simply choose a value of q^* with a sufficiently high distortion energy and minimise the energy with respect to all other primitive q internal coordinates. The steepest descent solution beginning at this initial geometry rapidly converges to a quasi-minimum energy path along the bottom of the PES valley leading to the nearest minimum, and the path solutions in the regions of interest change negligibly with adjustments to the initial boundary condition.

2.3. RAS embedding

Vibrational and rotational motion are non-separable owing to Coriolis coupling in the molecular KEO. Quantifying the magnitude of rovibrational coupling can be a subtle question [24, 25], but for this discussion we simply focus on the off-diagonal matrix elements of the curvilinear metric tensor, $g_{\alpha i}$, between rotation about the molecular axis α and displacement of internal coordinate q_i . For a coordinate system defined by $\vec{x}_a(\mathbf{q})$, these tensor elements are

$$g_{\alpha i} = \sum_{a=1}^{N} m_a \left(\vec{x}_a \times \frac{\partial \vec{x}_a}{\partial q_i} \right)_{\alpha},$$

where a = 1, ..., N labels the N atoms with masses m_a [26]. The well known Eckart conditions [20] require that $\vec{x}_a(\mathbf{q})$ satisfy

$$\sum_{a=1}^{N} m_a(\vec{x}_{a,0} \times \vec{x}_a) = 0, \tag{2}$$

at a fixed reference geometry $\vec{x}_{a,0} = \vec{x}_a(\mathbf{q}_0)$ usually chosen to be the equilibrium geometry in its principal axis system. Differentiation of Equation (2) ensures that $g_{\alpha i} =$ 0 at the reference geometry and therefore remains small for small-amplitude vibrations about it. It will be useful later to note that an equivalent definition of the Eckart frame is that in which the mass-weighted squareddistance between $\vec{x}_a(\mathbf{q})$ and the reference geometry $\vec{x}_{a,0}$, i.e.

$$\sum_{a=1}^{N} m_a |\vec{x}_{a,0} - \vec{x}_a|^2, \tag{3}$$

is minimised with respect to rotations of \vec{x}_a [27–29].

The benefit of the Eckart conditions diminishes for large-amplitude displacements, in which case Equation (2) no longer guarantees that $g_{\alpha i}$ remains small. An early solution to the large-amplitude problem was introduced by Sayvetz [30]. Here, we adopt the closely related

approach of Pickett [8], who observed that a more general choice of molecule-fixed frame, the so-called reduced axis system, or RAS, can be chosen to satisfy $g_{\alpha i} = 0$ for arbitrary displacements of a single large-amplitude vibration, q^* . For example, in one dimension, given some initial frame embedding defined by $\vec{x}_a(q^*)$ for which $g_{\alpha i} \neq$ 0, we define a 3 \times 3 orthogonal rotation matrix $R(q^*)$ that moves \vec{x}_a into a new frame $\vec{x}_a' = R(q^*)\vec{x}_a(q^*)$. The three independent constraints

$$\sum_{a=1}^{N} m_a \left(R(q^*) \vec{x}_a(q^*) \times \frac{\partial (R(q^*) \vec{x}_a(q^*))}{\partial q^*} \right)_{\alpha} = 0 \quad (4)$$

for each molecule-fixed axis α define a set of coupled differential equations for the three independent matrix elements of the orthogonal matrix $R(q^*)$. In other words, $R(q^*)$ rotates the molecule to exactly cancel the vibrational angular momentum that would be generated by motion of q^* in the original frame. In cases for which axial or planar symmetry is conserved everywhere along the one-dimensional q^* path, two components of Equation (4) are trivially satisfied, and the problem reduces to a single differential equation for the rotation angle about the unique axis [8]. In both the general and these special cases, it is straightforward to compute $R(q^*)$ by numerical integration or power series solution of Equation (4), so long as the functions $\vec{x}_a(q^*)$ and their derivatives can be calculated [8].

The RAS conditions ensure that Coriolis coupling between the large-amplitude coordinate q^* and each rotation axis is identically zero everywhere along a one-dimensional path, which we choose here to be the RP defined above. To remove Coriolis coupling with the small-amplitude orthogonal displacements, d_i , we further require that modified Eckart conditions are also satisfied with respect to these displacements and a moving reference geometry defined by the initial RAS rotation along the reaction path, i.e. the geometry $\vec{x}_a'(q^*, \mathbf{d} = 0) = R(q^*)\vec{x}_a(q^*, \mathbf{d} = 0)$ that satisfies Equation (4). These moving Eckart conditions are imposed by adapting the mass-weighted squareddistance expression above (Equation (3)) to account for a moving reference geometry,

$$\sum_{a=1}^{N} m_a |\vec{\mathbf{x}}_a'(q^*, \mathbf{d} = 0) - \vec{\mathbf{x}}_a'(q^*, \mathbf{d})|^2.$$
 (5)

The molecule-fixed frame coordinates that minimise this quantity for arbitrary d are found using quaternion algebra [29], which is straightforward to adapt to a moving Eckart reference geometry [1, 6]. This final RAS frame ensures that $g_{\alpha i} = 0$ for both the large- and small-amplitude coordinates everywhere along the onedimensional RP.

In the original formulation of the RP Hamiltonian [2], the RAS conditions were automatically satisfied because the RP was derived from the beginning with respect to mass-weighted Cartesian energy gradients, which induce zero angular momentum owing to the rotational invariance of the potential energy, while the moving Eckart conditions were explicitly met by simple constraints placed on the orthogonal normal modes defined with respect to mass-weighted rectilinear displacements (Equations 4.3 and 4.4 in [2]). Rovibrational calculations based directly on this conventional RP Hamiltonian, e.g. the variational vibrational configuration interaction (VCI) calculations of H₂O₂ by Carter et al. [5], therefore already offer a demonstration of the benefits of the RP-RAS approach to rotating molecules undergoing large-amplitude motion. The consideration of general curvilinear primitive coordinate systems (and the resulting RP displacement coordinates) as the starting point here requires the somewhat more elaborate procedures discussed above to meet these same conditions.

3. Results

We now illustrate the application of the RP-RAS Hamiltonian for rovibrational VMP2 parameters using reduceddimension models of two examples of large-amplitude tunnelling motions: internal rotation in hydrogen peroxide and inversion tunnelling in cyclopropyl radical. The primary aim is to compare whether the RAS frame embedding has a significant effect on the accuracy of VMP2 predictions relative to standard Eckart embeddings using various reference geometries. Reference values for the effective Hamiltonian parameters for these small model systems are easily computed with highly converged, numerically exact variational calculations (using the same underlying DVR basis sets for meaningful comparison). The variational and VMP2 calculations, as well as all of the preliminary RP and RAS calculations, are performed with the NITROGEN program package [31], which implements a number of automatic differentiation tools that simplify the somewhat elaborate chain of RP, RAS, and Eckart coordinate system transformations described above. The PES functions are taken from published sources or calculated in this work as described below for each example.

3.1. Torsional tunnelling in hydrogen peroxide

Hydrogen peroxide, H₂O₂, is a classical example of largeamplitude internal rotation tunnelling [6, 32-43]. It has two mirror-image bent equilibrium configurations separated by a planar trans transition state (TS) with a

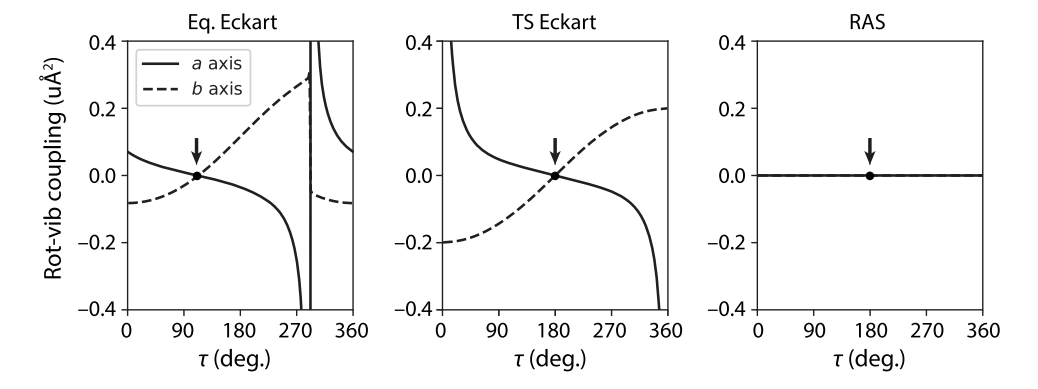


Figure 1. Rovibrational coupling coefficients in different H_2O_2 frame embeddings. The g metric tensor component between the antisymmetric HOO bending normal mode (b_u symmetry) and rotation about the a (solid line) and b (dashed line) axes is plotted along the reaction path parameterised by the τ (HOOH) torsion angle. (This mode does not couple to the c axis by symmetry.) The equilibrium Eckart, TS Eckart, and RAS frames are shown in the left, middle, and right panels, respectively. The a and b axes correspond to the instantaneous principal axes at the reference geometry indicated by the arrow.

low energy height ($\sim 390\,\mathrm{cm}^{-1}$) and a much higher cis barrier ($\sim 2500 \, \mathrm{cm}^{-1}$) [39]. The present calculations use the high-quality PES calculated by Małyszek and Koput [43]. Following the procedures outlined above, the isomerisation RP Hamiltonian was calculated beginning with a primitive internal coordinate system comprising the six valence coordinates: the three sequential bond lengths, the two HOO bond angles, and the HOOH dihedral angle, τ . Three different frame embeddings were used for rovibrational VMP2 calculations: (i) a standard Eckart frame using one of the two equivalent minima as the reference geometry ('equilibrium Eckart'), (ii) a standard Eckart frame using the trans transition state as the reference geometry ('TS Eckart'), and (iii) the RAS frame. (The RAS frame defined by Equation (4) requires an arbitrary initial point for integration, which was chosen here to be the principal axis system of the trans TS geometry at $\tau = 180^{\circ}$.) Figure 1 shows a representative subset of the rovibrational coupling coefficients $g_{\alpha i}$ along the RP in each of these frames.

The variational and VMP2 rovibrational parameters were calculated with these Hamiltonians after freezing the two highest-frequency RP normal modes (i.e. the symmetric and antisymmetric OH stretches) to zero displacement. Table 1 summarises the rotational constants A, B, and C for the lower $(A_0, \text{ etc.})$ and upper $(A_1, \text{ etc.})$ components of the ground-state torsion tunnelling doublet. The reference values were derived by least-squares optimising a rigid rotor Hamiltonian, $H = AJ_a^2 + BJ_b^2 +$ CJ_c^2 , to the variational energies of each tunnelling component for $J \leq 2$. The absolute value of each rotational constant is reported for the variational reference results, and the difference of the corresponding parameter is shown for the three sets of rovibrational VMP2 predictions. The 'single-state VMP2' rotational constants are calculated with VSCF solutions optimised separately for

Table 1. Effective rotational constants of the lowest tunnelling doublet of a four-dimensional model of H_2O_2 .

		Single-state VMP2					
Parameter	Reference ^a	Equilibrium Eckart	TS Eckart	RAS			
$\overline{A_0}$	10.31208(6)	+100.58591	-0.00368	+0.00042			
B ₀	0.87584(8)	+0.31496	-0.00013	-0.00001			
C_0	0.83879(8)	-0.48584	-0.00014	-0.00004			
A ₁	10.30609(7)	+127.95791	-0.00619	+0.00051			
B_1	0.87379(9)	+0.37219	-0.00029	+0.00005			
C ₁	0.84188(9)	-0.57567	-0.00009	+0.00001			

Note: All values are in cm $^{-1}$.a Reference values derived from rigid-rotor fits to variational $J \leq 2$ energies. The standard 1σ least-squares fit uncertainties are shown in parentheses in units of the last digit.

each of the lower and upper tunnelling states. Their values are determined directly from the rovibrational VMP2 contact transformation (see Ref. [1]) without the need for least-squares fitting.

The rovibrational VMP2 predictions using the three different frame embeddings show systematic differences in performance. The Eckart frame referenced to the equilibrium geometry at $\tau \approx 112^{\circ}$ has nonphysically large errors owing to a Coriolis singularity near $\tau \approx$ 290°, as is apparent in Figure 1. At this geometry, the Eckart conditions have multiple solutions, which demonstrates a general difficulty for standard Eckart embeddings with large-amplitude motion. This problem is partially circumvented in the TS Eckart frame, where the reference configuration is the trans TS at $\tau = 180^{\circ}$. It shows the same type of singularity, but it occurs at $\tau = 0^{\circ}$. The present calculations avoid this singularity by using a τ DVR grid that extends only from 5° to 355°, and the TS Eckart frame in fact already provides highly accurate vibrationally averaged rotational constants for both ground-state tunnelling components, the fractional errors being of order 10^{-3} to 10^{-4} . The RAS frame, nonetheless, shows further systematic

improvement, with errors decreased by another order of magnitude. All three VMP2 calculations yield identical values for the tunnelling doublet splitting because the pure vibrational part of the Hamiltonian is invariant to the molecule-fixed frame embedding. The VMP2 tunnelling energy for the four-dimensional RP Hamiltonian is 14.395 cm⁻¹, in excellent agreement with the variational reference value, $14.400 \, \text{cm}^{-1}$.

3.2. Inversion motion in cyclopropyl radical

The cyclopropyl radical, c-C₃H₅, is formed by homolytic cleavage of the CH bond of cyclopropane. It has two mirror-image equilibrium configurations with the α -H atom bent above or below the C-C-C plane by $\pm 40^{\circ}$ [44–49]. These two minima are separated by a $C_{2\nu}$ TS with a barrier height of approximately 1000 cm⁻¹, giving rise to a ground-state inversion tunnelling splitting of 3-4 cm⁻¹ [44]. A three-dimensional model PES for cyclopropyl was constructed by fitting a grid of singlepoint energies calculated at the CCSD(T)/cc-pVDZ level of theory [50–52]. The grid included the α -CH bond length $(r \in [0.8 \text{ Å}, 1.2 \text{ Å}]$ in steps of 0.08 Å), the inversion bending angle ($\theta \in [-60^{\circ}, +60^{\circ}]$ in steps of 5°), and the perpendicular CH 'wagging' angle ($\phi \in [60^{\circ}, 120^{\circ}]$

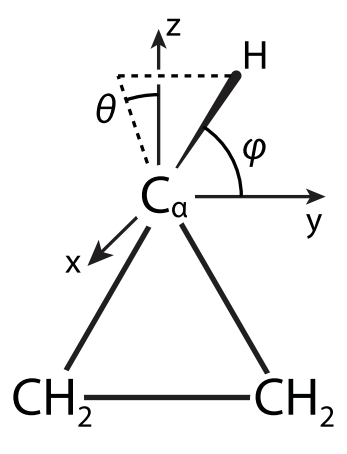


Figure 2. The bending coordinates (θ, ϕ) in the reduceddimension model of c- C_3H_5 . The C_3 skeleton defines the yz plane.

in steps of 10°). (The angle coordinates are defined in Figure 2.) At each point, all other structural parameters were optimised to the minimum constrained energy. The energy grid was then used to fit to a sextic polynomial in the (r, θ, ϕ) coordinates (rms fit residual = 8 cm⁻¹). The RP-RAS coordinate system was calculated in this reduced-dimension model as described above using the $C_{2\nu}$ TS geometry (i.e. $\theta = 0^{\circ}, \phi = 90^{\circ}$) as the RAS initial integration point. The equilibrium and TS Eckart frames are free of the types of singularities observed in the H₂O₂ example because the c-C₃H₅ Eckart axes remain more or less aligned with respect to the heavy C₃ skeleton for all values of the inversion coordinate θ .

The rotational constants for the ground-state inversion doublet are summarised in Table 2. The first set of predictions is based on the single-state VMP2 rotational Hamiltonians calculated in the same manner as for H_2O_2 . The two tunnelling components in cyclopropyl, however, have a symmetry allowed a-type off-diagonal Coriolis interaction, parameterised as $F_{01}(J_bJ_c + J_cJ_b)$ [8]. The single-state VMP2 effective Hamiltonians neglect this vibrationally off-diagonal interaction, but it can be captured by a two-state VMP2 Hamiltonian that includes both tunnelling components simultaneously [1]. In this case, the unreduced two-state rovibrational VMP2 Hamiltonians are explicitly diagonalised and the rovibrational energies ($J \le 2$) are used to re-fit the same reduced two-state Hamiltonian used for the variational reference values, i.e.

$$H = \begin{bmatrix} A_0 J_a^2 + B_0 J_b^2 + C_0 J_c^2 & F_{01} (J_b J_c + J_c J_b) \\ F_{01} (J_b J_c + J_c J_b) & \Delta E + A_1 J_a^2 + B_1 J_b^2 + C_1 J_c^2 \end{bmatrix}.$$
(6)

The errors of these two-state results are included in the last three columns of Table 2. The RAS embedding shows the best performance, particularly for the 'proper' two-state Hamiltonian, the RAS errors of which are generally an order of magnitude smaller than either of the single-reference Eckart frames. The fractional accuracy is below 10^{-4} for both the rotational constants and the F_{01} tunnelling-rotation parameter. The tunnelling

Table 2. Effective rotational constants of the lowest tunnelling doublet of a three-dimensional model of $c-C_3H_5$.

		Single-state VMP2			Two-state VMP2			
Parameter	Reference ^a	Equilibrium Eckart	TS Eckart	RAS	Equilibrium Eckart	TS Eckart	RAS	
$\overline{A_0}$	23706.558(3)	-2.494	-3.232	-0.917	-0.359(8)	-1.077(7)	+0.055(3)	
B ₀	20754.466(3)	+6.902	+2.333	+0.771	+5.210(8)	+0.501(7)	+0.053(3)	
C_0	13204.788(2)	-0.597	+1.004	+0.497	-1.202(6)	+0.065(5)	-0.121(2)	
A ₁	23712.575(3)	+1.150	+1.099	+1.059	-1.168(8)	-1.214(7)	+0.037(3)	
B ₁	20748.090(3)	+4.315	-0.715	-0.581	+5.170(9)	+0.358(7)	+0.026(3)	
C ₁	13208.502(3)	-2.918	-1.781	-0.829	-1.239(10)	+0.040(8)	-0.121(4)	
F ₀₁	156.884(179)	_	_	-	+1.160(487)	+1.722(400)	+0.005(179)	

Note: All values are in MHz. ^a Reference values derived from fitting the two-state model (Equation (6)) to the variational $J \le 2$ energies. The standard 1σ leastsquares fit uncertainties are shown in parentheses in units of the last digit.



splittings calculated with either the single-state VMP2 (78,135 MHz) or two-state VMP2 (78,140 MHz) models are also in excellent agreement with the variational reference value (78,151 MHz). [Note that the nominal fit uncertainties reported in Table 2 for the reference and two-state rotational parameters do not necessarily reflect the meaningful limit of comparison. For example, the difference between the reference and two-state RAS-VMP2 values for F_{01} is $\sim 35 \times$ smaller than the nominal 1σ fit uncertainty, but this uncertainty reflects a systematic deficiency of the fitted model (i.e. neglect of centrifugal distortion) that is entirely common to the two fits.]

4. Discussion

The model results demonstrate that the RP-RAS Hamiltonian is well suited for rovibrational VMP2 calculations. Although the simpler TS Eckart embedding for both H₂O₂ and c-C₃H₅ is by no means a poor choice (at least for the ground-state rotational parameters), the RAS embedding generally decreases the errors of these parameters by an order of magnitude. Reduced-dimension models were used in this study so that reference variational results could be computed without significant computational effort, but a full-dimensional treatment will ultimately be needed for quantitative predictions that are useful for high-resolution microwave and optical spectroscopy. (For example, the tunnelling splitting of the 4-D H₂O₂ model is 14.4 cm⁻¹, which is 30% larger than the full-dimensional value (11.0 cm^{-1}) for this PES [43]. The measured value is $11.4\,\mathrm{cm}^{-1}$ [39].) Full-dimensional VMP2 calculations can be extended to larger systems by using truncated many-body expansions of the molecular Hamiltonian [53, 54], which have performed well in our previous applications of VMP2 to non-rigid molecules with up to 24 vibrational modes [1, 6, 7] and in other VSCF-VCI applications with large-amplitude motion including that of H_2O_2 and CH_3OH [3–5]. (Such many-body expansions not yet been implemented into the code for the present RP-RAS-VMP2 calculations.) The VMP2 approach also performs well for vibrationally excited states, so long as they are isolated or belong to a small polyad of interacting states that can be modelled by a modestly sized multi-state effective Hamiltonian [1, 6]. Nonetheless, given that both TS Eckart and RAS embeddings have fractional errors of 10^{-3} or smaller, which is approximately the minimum error for ab initio rotational parameters achievable by electronic structure calculations of medium-sized molecules [55], it is reasonable to question whether the RAS Hamiltonian is worth the extra effort.

The singularities observed in the H₂O₂ rovibrational KEO coefficients (Figure 1) illustrate one of the

comparative advantages of the RAS frame. The position of the singularity in the equilibrium Eckart frame made it entirely unsuitable for large-amplitude torsion calculations. This issue could be avoided for the TS Eckart embedding only because we have focussed on the ground-state tunnelling-rotation parameters, and the location of the singularity ($\tau = 0^{\circ}$) is energetically unimportant for these predictions. This approximation cannot be made, however, for torsionally excited states that sample all values of τ . The RAS frame removes most of these difficulties, but we must point out, however, that our implicit choice of boundary condition for the RAS rotation matrix $R(\tau)$ has a discontinuity at $\tau = 0^{\circ}$, i.e. $R(0^{\circ}) = -R(360^{\circ})$. Torsionally excited calculations in the RAS frame would need to either introduce a non-zero average value for some $g_{i\alpha}$ tensor elements or introduce modified periodic boundary conditions [8]. These considerations are relevant to other related embeddings for periodic motion including the internal-axis and ρ -axis systems [56-58], and these ideas could be incorporated into the rovibrational VMP2 framework. Other types of multi-reference Eckart frames [59, 60] provide a similar route to approximate rotation-vibration separability with large-amplitude motion, and it would be interesting to evaluate how well rovibrational VMP2 performs with these types of embeddings.

An important conceptual and computational advantage of the RP-RAS Hamiltonian is that it brings the microscopic molecular Hamiltonian much closer to the empirical reduced effective Hamiltonian used implicitly when fitting experimentally measured spectroscopic transition frequencies. For example, for the two-state tunnelling-rotation Hamiltonian used here for cyclopropyl (and, indeed, for many other inversiontunnelling and ring-puckering systems, e.g. dimethylamine [61], gauche-1,3-butadiene [7], glycinamide [62], ammonia [63], ethylene glycol [64], cyclopentene [65], and tetrahydrofuran [66–68]), the choice of a $F_{01}(J_bJ_c +$ J_cJ_b)-type interaction term instead of a momentum-type interaction ($\sim J_a \partial_\theta$) can also be viewed as a choice of Hamiltonian reduction equivalent to defining the molecule-fixed axes as those of the RAS frame, hence the name 'reduced' axis system [8]. Rotational quantum numbers [69, 70] and various vector- and tensor-valued properties that are defined with respect to molecule-fixed axes (e.g. dipole moments, spin-rotation coupling tensors, electric field gradients, and other hyperfine parameters) are therefore influenced by this choice of reduction, and computing and interpreting these quantities requires a careful consideration of the implicit or explicit axis system of a given effective Hamiltonian. As described above, the reduced tunnelling-rotation parameters for the two-state cyclopropyl Hamiltonians in Table 2 were derived by first diagonalising the unreduced Hamiltonian provided directly by VMP2 [1] and then re-fitting the eigenenergies with the reduced form of the Hamiltonian (Equation (6)). The difference or similarity of the unreduced VMP2 rotational parameters with the fitted reduced values quantifies how close each embedding corresponds to the implicit axes of the empirical RAS effective Hamiltonian. For the cyclopropyl example, the equilibrium Eckart, TS Eckart, and RAS embeddings have unreduced F₀₁ values of 215.5, 179.9, and 156.1 MHz, respectively, which are to be compared with the variational reference value of 156.9 MHz. As anticipated, the unreduced F_{01} parameter for the RAS embedding is nearly equal to the reference reduced value because the microscopic RP-RAS Hamiltonian already closely mirrors the axis system implicit in the empirical Hamiltonian.

The VSCF zeroth-order solution clearly provides a suitable starting point for perturbation theory-based effective Hamiltonians, but it is worth considering whether even simpler zeroth-order wavefunctions could be used. For example, instead of solutions to the onebody VSCF mean-field Hamiltonians, one could adopt solutions to one-dimensional 'cuts' along RP coordinates. We do not explore this alternative further here, but one potential difficulty with this approach could be deciding where to take the cut (which is a stronger restriction of the zeroth-order wavefunction than that of VSCF). For large-amplitude motion between two equivalent wells, for example, cuts centred at either equilibrium geometry might neglect aspects of the full molecular symmetry, while taking cuts at a symmetrically located TS might ignore the more relevant features of the PES near the equilibrium geometry where the ground-state wavefunction has most of its amplitude. From this perspective, VSCF is a convenient hands-off procedure for performing 'averaged cuts' that preserve molecular symmetry and weight the most important geometric configurations. In a similar vein, while the focus of this study is the comparative performance of different embeddings on VMP2 predictions, it would be interesting to explore alternatives to the RP coordinate system itself, e.g. one based on instanton paths that provide a semi-classically optimal description of tunnelling [71], or to coordinate systems for two or more simultaneous large-amplitude degrees of freedom [72, 73].

5. Conclusions

The RP-RAS Hamiltonian provides an efficient representation of molecular motion in which one-dimensional large-amplitude motion, small-amplitude displacements, and molecular rotations are highly mutually separable.

The RAS embedding systematically improves the accuracy of rovibrational parameters calculated by curvilinear VMP2 compared to those with Eckart frames referenced to equilibrium or TS geometries. The close relationship between the microscopic RP-RAS Hamiltonian and the empirical effective Hamiltonians commonly used for tunnelling-rotating molecules may simplify the calculation and interpretation of vibrationally averaged ground-state properties. The modest computational cost of VMP2 makes this a promising scheme for high-accuracy *ab initio* tunnelling-rotation calculations of large molecules not otherwise achievable by more expensive nuclear motion methods.

Note

1. This local condition can also be met with other related embedding schemes that differ from the Eckart frame for non-infinitesimal displacements [74].

Acknowledgments

The author is delighted to contribute this paper in honour of Prof. Attila Császár, whose extensive body of work on the motion of 'floppy' molecules of all kinds is a valued source of insight, instruction, and inspiration.

Disclosure statement

No potential conflict of interest was reported by the author(s).

Funding

This work was supported by the U.S. National Science Foundation under Awards PHY-2110489 and AST-1908576.

ORCID

P. Bryan Changala http://orcid.org/0000-0003-0304-9814

References

- [1] P.B. Changala and J.H. Baraban, J. Chem. Phys. **145**, 174106 (2016). doi:10.1063/1.4966234.
- [2] W.H. Miller, N.C. Handy and J.E. Adams, J. Chem. Phys. **72**, 99 (1980). doi:10.1063/1.438959.
- [3] S. Carter and N.C. Handy, J. Chem. Phys. **113**, 987–993 (2000). doi:10.1063/1.481879.
- [4] J.M. Bowman, X. Huang, N.C. Handy and S. Carter, J. Phys. Chem. A 111, 7317–7321 (2007). doi:10.1021/ jp070398m.
- [5] S. Carter, A.R. Sharma and J.M. Bowman, J. Chem. Phys. 135, 014308 (2011). doi:10.1063/1.3604935.
- [6] J.H. Baraban, P.B. Changala and J.F. Stanton, J. Mol. Spectrosc. **343**, 92–95 (2018). doi:10.1016/j.jms.2017.09.014.
- [7] J.H. Baraban, M.A. Martin-Drumel, P.B. Changala, S. Eibenberger, M. Nava, D. Patterson, J.F. Stanton, G.B. Ellison and M.C. McCarthy, Angew. Chem. Int. Ed. 57, 1821–1825 (2018). doi:10.1002/anie.v57.7.

- [8] H.M. Pickett, J. Chem. Phys. 56, 1715 (1972). doi:10.1063/
- 1.1677430. [9] L.S. Norris, M.A. Ratner, A.E. Roitberg and R.B. Gerber, J. Chem. Phys. 105, 11261-11267 (1996). doi:10.1063/1.
- [10] O. Christiansen, J. Chem. Phys. 119, 5773-5781 (2003). doi:10.1063/1.1601593.
- [11] J.O. Jung and R.B. Gerber, J. Chem. Phys. 105, 10332 (1996). doi:10.1063/1.472960.
- [12] J.M. Bowman, J. Chem. Phys. **68** (2), 608–610 (1978). doi:10.1063/1.435782.
- [13] R.B. Gerber and M.A. Ratner, Adv. Chem. Phys. 70, 97-132 (1988).
- [14] J.C. Light and T. Carrington Jr., Adv. Chem. Phys. 114, 263-310 (2000).
- [15] N. Matsunaga, G.M. Chaban and R.B. Gerber, J. Chem. Phys. 117, 3541-3547 (2002). doi:10.1063/1.1494978.
- [16] I.M. Mills, in Molecular Spectroscopy: Modern Research, edited by K. Narahari Rao and C. Weldon Mathews, (Academic Press, New York, 1972), Chap. 3.2, pp. 115-
- [17] J.K.G. Watson, in Vibrational Spectra and Structure, edited by J. Durig, (Elsevier, Amsterdam, 1977), Vol. 6,
- [18] J.K.G. Watson, Mol. Phys. 15, 479-490 (1968). doi:10. 1080/00268976800101381.
- [19] E.B. Wilson Jr., J.C. Decius and P.C. Cross, Molecular Vibrations (Dover, New York, 1955).
- [20] C. Eckart, Phys. Rev. 47, 552-558 (1935). doi:10.1103/ PhysRev.47.552.
- [21] G.A. Natanson, B.C. Garrett, T.N. Truong, T. Joseph and D.G. Truhlar, J. Chem. Phys. 94, 7875-7892 (1991). doi:10.1063/1.460123.
- [22] M. Page, C. Doubleday and J.W. McIver, J. Chem. Phys. 93, 5634-5642 (1990). doi:10.1063/1.459634.
- [23] A. Nauts and X. Chapuisat, Chem. Phys. 76, 349-366 (1983). doi:10.1016/0301-0104(83)85218-5.
- [24] J. Sarka, B. Poirier, V. Szalay and A.G. Császár, Sci. Rep. 10, 4872 (2020). doi:10.1038/s41598-020-60971-x.
- [25] J. Sarka, B. Poirier, V. Szalay and A.G. Császár, Spectrochim. Acta A: Mol. Biomol. Spectrosc. 250, 119164 (2021). doi:10.1016/j.saa.2020.119164.
- [26] R. Meyer and H.H. Günthard, J. Chem. Phys. 49, 1510-1520 (1968). doi:10.1063/1.1670272.
- [27] F. Jørgensen, Int. J. Quant. Chem. 14, 55-63 (1978). doi:10.1002/qua.v14:1.
- [28] K.N. Kudin and A.Y. Dymarsky, J. Chem. Phys. 122, 224105 (2005).
- [29] S.V. Krasnoshchekov, E.V. Isayeva and N.F. Stepanov, J. Chem. Phys. 140, 154104 (2014). doi:10.1063/1.4870936.
- [30] A. Sayvetz, J. Chem. Phys. 7, 383 (1939). doi:10.1063/1. 1750455.
- [31] P.B. Changala, *NITROGEN*, version 2.1.2 (2021). https:// github.com/bchangala/nitrogen, doi:10.5281/zenodo. 7342277.
- [32] J.T. Hougen, Can. J. Phys. 62, 1392-1402 (1984). doi:10. 1139/p84-186.
- [33] J.T. Massey and D.R. Bianco, J. Chem. Phys. 22, 442-448 (1954). doi:10.1063/1.1740088.
- [34] R.L. Redington, W.B. Olson and P.C. Cross, J. Chem. Phys. 36, 1311-1326 (1962). doi:10.1063/1.1732733.

- [35] G.A. Khachkuruzov and I.N. Przhevalskii, Opt. Spektrosk. 36, 172-174 (1974).
- [36] D. Cremer and D. Christen, J. Mol. Spectrosc. 74, 480–482 (1979). doi:10.1016/0022-2852(79)90169-3.
- [37] P. Helminger, W.C. Bowman and F.C. De Lucia, J. Mol. Spectrosc. 85, 120-130 (1981). doi:10.1016/0022-2852(81)90314-3.
- [38] J. Koput, J. Mol. Spectrosc. 115, 438-441 (1986). doi:10. 1016/0022-2852(86)90058-5.
- [39] J.M. Flaud, C. Camy-Peyret, J.W.C. Johns and B. Carli, J. Chem. Phys. 91, 1504 (1989). doi:10.1063/1.457110.
- [40] J. Koput, Chem. Phys. Lett. 236, 516-520 (1995). doi:10.1016/0009-2614(95)00246-Z.
- [41] J. Koput, S. Carter and N.C. Handy, J. Phys. Chem. A 102, 6325-6330 (1998). doi:10.1021/jp9812583.
- [42] B. Kuhn, T.R. Rizzo, D. Luckhaus, M. Quack and M.A. Suhm, J. Chem. Phys. 111, 2565 (1999). doi:10.1063/1. 479534.
- [43] P. Małyszek and J. Koput, J. Comp. Chem. 34, 337-345 (2013). doi:10.1002/jcc.v34.5.
- [44] F. Dong, S. Davis and D.J. Nesbitt, J. Phys. Chem. A 110, 3059-3070 (2006). doi:10.1021/jp053994u.
- [45] N. Genossar, P.B. Changala, B. Gans, J.C. Loison, S. Hartweg, M.A. Martin-Drumel, G.A. Garcia, J.F. Stanton, B. Ruscic and J.H. Baraban, J. Amer. Chem. Soc. 144, 18518 (2022). doi:10.1021/jacs.2c07740.
- [46] R.W. Fessenden and R.H. Schuler, J. Chem. Phys. 39, 2147 (1963). doi:10.1063/1.1701415.
- [47] J.K. Kochi, P. Bakuzis and P.J. Krusic, J. Amer. Chem. Soc. 95, 1516–1526 (1973). doi:10.1021/ja00786a029.
- [48] V. Barone, C. Minichino, H. Faucher, R. Subra and A. Grand, Chem. Phys. Lett. 205, 324-330 (1993). doi:10.1016/0009-2614(93)89250-L.
- [49] M. Dupuis and J. Pacansky, J. Chem. Phys. 76, 2511–2515 (1982). doi:10.1063/1.443282.
- [50] K. Raghavachari, G.W. Trucks, J.A. Pople and M. Head-Gordon, Chem. Phys. Lett. 157, 479-483 (1989). doi:10.1016/S0009-2614(89)87395-6.
- [51] R.J. Bartlett, J. Watts, S. Kucharski and J. Noga, Chem. Phys. Lett. 165, 513-522 (1990). doi:10.1016/0009-2614 (90)87031-L.
- [52] T.H. Dunning, J. Chem. Phys. 90, 1007 (1989). doi:10. 1063/1.456153.
- [53] S. Carter, S.J. Culik and J.M. Bowman, J. Chem. Phys. 107, 10458-10469 (1997). doi:10.1063/1.474210.
- [54] D. Strobusch and C. Scheurer, J. Chem. Phys. 135, 124102 (2011). doi:10.1063/1.3637629.
- [55] Z.N. Heim, B.K. Amberger, B.J. Esselman, J.F. Stanton, R.C. Woods and R.J. McMahon, J. Chem. Phys. 152, 104303 (2020). doi:10.1063/1.5144914.
- [56] C.C. Lin and J.D. Swalen, Rev. Mod. Phys. **31** (4), 841–892 (1959). doi:10.1103/RevModPhys.31.841.
- [57] V. Szalay and J. Ortigoso, J. Chem. Phys. 109, 3911–3918 (1998). doi:10.1063/1.476990.
- [58] V. Szalay, A.G. Császár, J. Santos and J. Ortigoso, J. Chem. Phys. 118, 6801-6805 (2003). doi:10.1063/1.1560634.
- [59] D. Lauvergnat, J.M. Luis, B. Kirtman, H. Reis and A. Nauts, J. Chem. Phys. 144, 084116 (2016). doi:10.1063/1. 4942172.
- [60] X.G. Wang and T. Carrington, J. Chem. Phys. 138, 104106 (2013). doi:10.1063/1.4793474.



- [61] H.S.P. Müller, R.T. Garrod, A. Belloche, V.M. Rivilla, K.M. Menten, I. Jiménez-Serra, J. Martín-Pintado, F. Lewen and S. Schlemmer, Mon. Not. R. Astron. Soc. 523, 2887–2917 (2023). doi:10.1093/mnras/stad1549.
- [62] Z. Kisiel, L. Kolesniková, A. Belloche, J.C. Guillemin, L. Pszczółkowski, E.R. Alonso, R.T. Garrod, E. Białkowska-Jaworska, I. León, H.S.P. Müller, K.M. Menten and J.L. Alonso, Astron. Astrophys. 657, A99 (2022). doi:10.1051/0004-6361/202142350.
- [63] E. Cohen and H. Pickett, J. Mol. Spectrosc. **93**, 83–100 (1982). doi:10.1016/0022-2852(82)90276-4.
- [64] H.S. Müller and D. Christen, J. Mol. Spectrosc. 228, 298–307 (2004). doi:10.1016/j.jms.2004.04.009.
- [65] J.C. López, J.L. Alonso, M. Charro, G. Wlodarczak and J. Demaison, J. Mol. Spectrosc. 155, 143–157 (1992). doi:10.1016/0022-2852(92)90554-2.
- [66] D.G. Melnik, S. Gopalakrishnan, T.A. Miller and F.C. De Lucia, J. Chem. Phys. 118, 3589–3599 (2003). doi:10.1063/1.1538241.

- [67] G.G. Engerholm, A.C. Luntz, W.D. Gwinn and D.O. Harris, J. Chem. Phys. 50, 2446–2457 (1969). doi:10.1063/1. 1671401.
- [68] R. Meyer, J.C. López, J.L. Alonso, S. Melandri, P.G. Favero and W. Caminati, J. Chem. Phys. 111, 7871–7880 (1999). doi:10.1063/1.480122.
- [69] T. Szidarovszky, C. Fábri and A.G. Császár, J. Chem. Phys. 136, 174112 (2012). doi:10.1063/1.4707463.
- [70] C. Fábri, E. Mátyus and A.G. Császár, Spectrochim. Acta A 119, 84–89 (2014). doi:10.1016/j.saa.2013.03. 090.
- [71] J.E. Lawrence, J. Dušek and J.O. Richardson, J. Chem. Phys. 159, 014111 (2023), doi:10.1063/5.0155579.
- [72] T. Carrington and W.H. Miller, J. Chem. Phys. **81**, 3942–3950 (1984). doi:10.1063/1.448187.
- [73] T. Carrington and W.H. Miller, J. Chem. Phys. 84, 4364–4370 (1986). doi:10.1063/1.450058.
- [74] K.L. Mardis and E.L. Sibert III, J. Chem. Phys. 106, 6618 (1997). doi:10.1063/1.473658.